

# INTERNATIONAL SOCIETY FOR SOIL MECHANICS AND GEOTECHNICAL ENGINEERING



*This paper was downloaded from the Online Library of the International Society for Soil Mechanics and Geotechnical Engineering (ISSMGE). The library is available here:*

<https://www.issmge.org/publications/online-library>

*This is an open-access database that archives thousands of papers published under the Auspices of the ISSMGE and maintained by the Innovation and Development Committee of ISSMGE.*

*The paper was published in the proceedings of the 11<sup>th</sup> International Symposium on Field Monitoring in Geomechanics and was edited by Dr. Andrew M. Ridley. The symposium was held in London, United Kingdom, 4-7 September 2022.*

## Long-term monitoring of settlements below a transition zone in a railway structure

Kourosh NASROLLAHI, Jelke DIJKSTRA, Jens C.O. NIELSEN, and Magnus EKH

Chalmers University of Technology, Gothenburg, Sweden  
Corresponding author: Kourosh Nasrollahi ([Kourosh@chalmers.se](mailto:Kourosh@chalmers.se))

### Abstract

Settlement of ballast and subgrade is a common problem in ballasted railway tracks. In particular, in transition zones between two different track forms, a dip in longitudinal level often develops on the ballasted side. Without timely maintenance, this differential settlement may lead to damage to track components and deteriorated passenger comfort. To ensure the safety of railway operation and reduce maintenance costs, it is necessary to monitor the structural health of the transition zone in an economical manner and detect any operational changes at an early stage.

In recent years with the advancement of fibre-optic technologies, fibre Bragg grating (FBG) sensors have been more commonly used in structural health monitoring (SHM) due to their outstanding advantages. The wide range of FBG sensors, such as for the measurement of strain, displacement, temperature, and acceleration, can be used to acquire data over large distances with high resolution and accuracy. In this study, an FBG-based long-term monitoring arrangement, with a high temporal resolution, is developed to verify and calibrate a model for prediction of settlement in a transition zone. The system is designed to measure an operational railway track in harsh conditions in the north of Sweden. Furthermore, the instrumentation comprises four clusters, each with an optical strain gauge array in the rail web, an accelerometer on the sleeper, and a displacement transducer. Two additional accelerometers are installed far from the transition zone to measure a reference state. Combined, the data should not only provide details on the long-term settlements, but also the change in dynamic response it underpins.

Keywords: Transition zone, slab track, ballasted track, settlement, fibre Bragg grating (FBG) sensors

### 1. Introduction

In transition zones between two different railway track forms, there is a discontinuity in track structure leading to a gradient in track stiffness. Examples include transitions between different superstructures, e.g., slab track to ballasted track, and/or between different substructures, e.g., embankment to a bridge or tunnel structure. Differences in loading and support conditions at the interfaces between track superstructure and substructure on either side of the transition may lead to differential track settlement and an irregularity in longitudinal rail level soon after construction because of densification of ballast and consolidation in the subsoil. This results in an amplification of the dynamic traffic loading along the transition, contributing to the degradation process of the foundation and resulting in a further deterioration of vertical track geometry. Historically, the aim of the design of transition zones has involved minimising the difference in track stiffness between the ballasted track and the engineering structure. This is often achieved via a gradual increase/decrease in stiffness along the transition zone, for example using under sleeper pads (USP).

SHM has been introduced as a useful tool in railways, aiming to manage the asset by providing feedback on the current health state of various railway components. SHM increases the reliability of the structure and reduces maintenance costs by early detection of damage during the life of the infrastructure. Traditional sensing techniques/devices have been commonly employed to assess railway tracks. However, these approaches fail to fulfil the demands for low-cost, stable, long-term, and high-accuracy performance monitoring of modern railway infrastructure (Du et al., 2020). Some techniques, such as Digital Image Correlation (DIC), suffer from the complexity of bulky sensing equipment and are not practicable for long-distance monitoring (Du et al., 2020). To overcome these challenges, alternative, affordable and reliable devices are considered for the monitoring of railway infrastructure. Optical fibre sensors offer enormous advantages over conventional and other smart sensors due to their high sensitivity, small size, the potential for short and long-distance measurement, and so on. For example, Wang (Wang, 2015) attached two FBG sensors on the rail web, as a bi-directional device, to measure the longitudinal force in a high-speed railway line. A temperature compensation through calibration tests was conducted. Wheeler et al. (Wheeler et al., 2019) measured dynamic strains in a rail using Rayleigh backscattered, distributed optical fibre sensors. The field test instrumentation included a 7.5 m long section of rail with nylon-coated single-mode fibres installed on the rail web at 20 mm and 155 mm from the bottom of

the rail, respectively. A calibration test was performed by applying a static load on the rail with magnitude up to 140 kN and measuring the static strains using the OBR 4600 interrogator from Luna Ltd. Then, the ODiSI-B analyser was applied to capture dynamic strains of the cyclic loading at sampling frequency 0.5 Hz.

Wang (Wang, 2019) used a Satellite Synthetic Radar (InSAR) to provide a solution for consecutive structural health monitoring of a transition zone with bi-/tri-weekly data updates and millimetre-level precision. Additionally, a DIC device and a measuring coach were applied to measure the settlement along the transition zone. All three methods showed that the differential settlement close to the transition was higher than elsewhere. In the monitoring procedure developed by Paixão (Paixão, 2014), the shear deformation of the rail was measured to assess wheel loads, vertical displacement of the rail, rail–sleeper relative displacements, and vertical acceleration of the sleepers. Additionally, an additional rail displacement transducer was placed 40 m away from the transition and used as a reference.

This paper presents descriptions of the test site, a pre-test simulation model for prediction of settlement in a transition zone, and the detailed sensor set-up to be used for the field measurement of a transition zone considering the harsh conditions in the northern part of Sweden. Dynamics and static responses of the transition zone will be considered in different sleeper bays using four clusters of an FBG-based sensor setup.

## 2. Test site description

The Swedish heavy haul line Malmbanan is a single-track railway line in the northern part of Sweden. Traffic is dominated by iron ore freight trains with axle loads 30 tonnes operating from the mines in Kiruna and Malmberget to the ports in Narvik and Luleå. The bottom dumper wagons are designed to haul heavy loads of pellets, rock and other easily unloadable commodities. These freight cars are supported and guided by three-piece bogies. Small curve radii and steep gradients in combination with severe weather conditions, including snowstorms and temperatures down to  $-40^{\circ}\text{C}$ , put tremendous strains on infrastructure and rolling stock. The speed of the loaded heavy haul trains is 60 km/h. The line is also used by passenger trains at maximum speed 135 km/h and by other freight trains. The annual traffic load is of the order of 14 MGT (mega gross tonnes), and the number of axle passages (loaded and unloaded) is of the order of 850 000 per year. The track design includes 60 kg/m rails, rail fastenings with 10 mm resilient rail pads, and concrete sleepers designed for axle load 35 tonnes at sleeper distance 0.6 m. The settlement rate along Malmbanan varies significantly depending on the local conditions and properties of the subgrade. However, for a poor section of the track, a typical settlement rate is of the order of 1 mm/year (Nielsen, 2017; Nielsen et al., 2020).

To determine the properties of the layered substructure at the test site at Gransjö, a Multi-Surface Analysis of Surface Waves (MASW) measurement has been performed. The MASW survey was designed to acquire Rayleigh wave data using vertical geophones (4.5 Hz natural frequency). The input signal was generated by striking an 8 kg sledgehammer vertically on an iron plate. The recording time was 1.0 seconds, and the sampling interval was 250  $\mu\text{s}$ . Along each section of aligned geophones, the measurements were performed at 2.0 m intervals, resulting in eight measurements along two sections each 14 m in length, and 13 measurements along one 24 m long section (Trafikverket, 2020). The measured shear wave speed  $V_s$  is directly related to the small-strain shear modulus  $G_0 = \rho V_s^2$ , while the Young's modulus is given by  $E = 2\rho V_s^2 (1+\nu)$ . Table 1 lists a summary of the measured soil properties.

The field measurements of long-term performance of the transition zone between a Moulded Modular Multi-Blocks (3MB) slab-track and ballasted track on Malmbanan will commence in September 2022 and will be conducted in collaboration with the Swedish Transport Administration (Trafikverket) and ACCIONA. The pre-test planning and instrumentation are described in the following chapters.



**Figure 1:** (left) Geographical location of iron ore line (Malmbanan), (right) Overview of Gransjö test site.

| Layer            | $i$ | $H_i(m)$ | $\rho_i (kg/m^3)$ | $v_i$ | $V_{s,i} (m/s)$ | $E_i (MPa)$ |
|------------------|-----|----------|-------------------|-------|-----------------|-------------|
| Ballast          | 1   | 0.3      | 1800              | 0.2   | 125             | 67.5        |
| Sub-ballast      | 2   | 1        | 2100              | 0.3   | 175             | 161.7       |
| Subgrade layer 1 | 3   | 2        | 2100              | 0.25  | 300             | 472.5       |
| Subgrade layer 2 | 4   | 8        | 2100              | 0.25  | >400            | >800        |

**Table 1.** Measured properties of the substructure layers at Gransjö. From (Trafikverket, 2020).

### 3. Pre-test simulation model

A two-dimensional time-domain model, implemented in the in-house software DIFF, for the simulation of vertical dynamic vehicle-track interaction in a transition zone between two different track forms is presented in Fig. 2. DIFF is used to calculate vertical wheel-rail contact forces, rail and sleeper vibrations (displacements, velocities, and accelerations), and loads on sleepers that are transmitted either through the rail (rail seat loads) or acting at the interface with the ballast. Here, the simulation model is used for pre-test planning in terms of predicting appropriate positions for the sensors. The state-dependent and discretely supported track model is a finite element model with rigid boundaries at each rail end and at the lower connection point of each spring/damper model representing the foundation. The complete transition zone track model consists of two sections: the ballasted track and the 3MB slab track (48 m at the site). In the field test, the loaded trains are moving from a softer track section (ballasted track) to a stiffer one (3MB slab-track). The 3MB concept is a reinforced standard precast slab designed for both mixed traffic and high-speed traffic. The slab panels can be set up both on bituminous and concrete subgrade layers (Morales-Gamiz, 2017). The rail and slab are modelled by the Euler-Bernoulli beam theory. Each sleeper is simplified as a rigid mass. Rail pads and ballast/soil below each sleeper are represented by non-interacting discrete springs and viscous dampers. The slab track is supported by a viscously damped Winkler foundation. In this study, the iron ore vehicle is represented by one car body and two three-piece bogies, each consisting of a bolster (in this model, rigidly connected to the car body), two side frames and two wheelsets. The vehicle model in Fig. 2 has 14 DOFs. The contact between each wheel and rail is modelled using a non-linear Hertzian spring. For more details of the model, see (Nasrollahi et al., 2021).

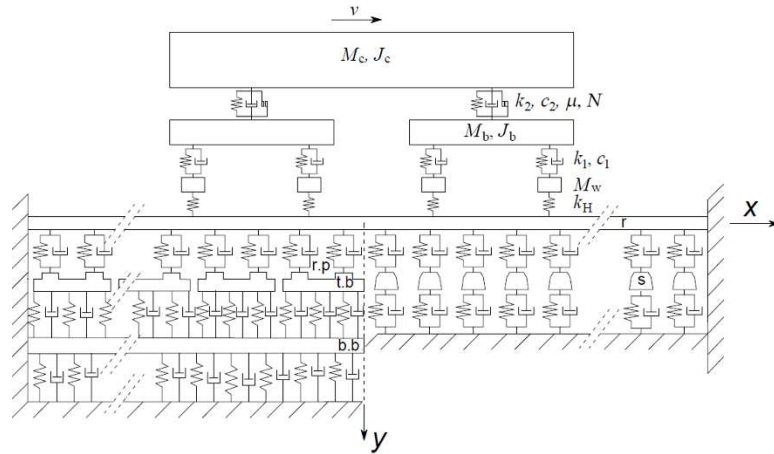


**Figure 2:** Principle sketch of vehicle and track models ( $x < 0$ : slab track,  $x > 0$ : ballasted track). The track model contains rail (r), top block (t.b) and base block (b.b) modelled by Euler-Bernoulli beam elements. The bottom block is supported by a Winkler foundation. The sleepers (s) are rigid masses supported by a spring-damper connection (representing the ballast/subgrade) with piecewise linear stiffness properties. The sleepers close to the transition ( $x = 0$ ) selected for long-term measurements are sleeper number 2, 5, 8, and 11.

The simulation procedure is based on an iterative approach where a time-domain model of dynamic vehicle-track interaction in the short-term is integrated with a model of accumulated ballast settlement in the long-term. The calculated load maxima at each interface between sleeper and ballast in the ballasted track section, generated by the combination of gravity load and the load induced by each of the wheels of the vehicle model, are used as input to a settlement model. The short-term model of the track dynamics is updated in each iteration step to account for the new states of the sleeper support conditions. By taking several iteration steps, the

accumulated (long-term) differential settlement and redistribution of foundation loads between adjacent sleepers are determined (Nasrollahi et al., 2021).

The empirical settlement model is based on a visco-plastic material model. For each wheel passage in each iteration step, the increment in settlement below a given sleeper is formulated as a function of the maximum generated sleeper–ballast contact pressure. This model assumes there is no incremental settlement if the maximum sleeper–ballast contact pressure is below a threshold value, which in each iteration step is dependent on the current level of accumulated settlement (Nasrollahi et al., 2021). The aim of the field measurement at Gransjö is to verify and calibrate this model of long-term differential settlement in a transition zone.

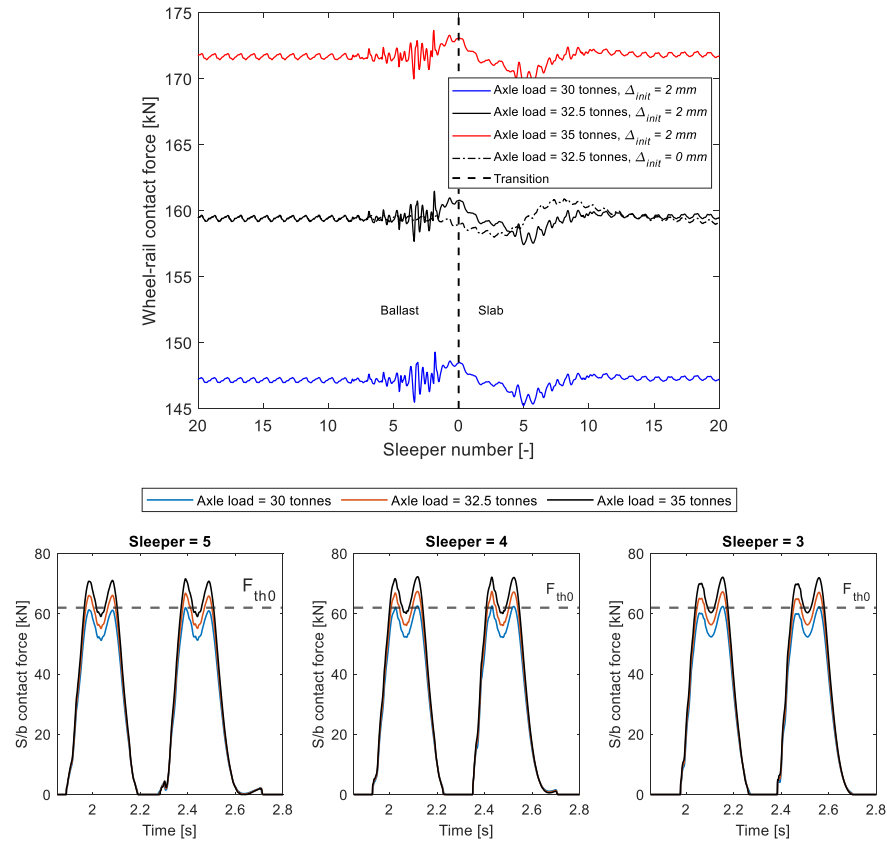


**Figure 3:** Influence of axle load on (top) wheel–rail contact force for the leading wheelset, with uniform initial settlement  $\Delta_{init} = 0$  or 2 mm of the ballasted track, and (bottom) sleeper–ballast contact force for sleepers 3 to 5 numbered from the transition. First iteration of the simulation procedure. From (Nasrollahi et al., 2021).

The wheel–rail contact force, sleeper–ballast force, sleeper acceleration, and the rail displacement due to gravity load after an accumulated traffic load of 14 MGT (one-year traffic load) have been computed by using DIFF (Nasrollahi et al., 2021). In the numerical simulations, a vehicle with speed 60 km/h and axle loads 30, 32.5, or 35 tonnes was considered. To represent the early densification of the ballast, a uniform initial misalignment in vertical level between the different track forms has been assumed by prescribing a uniform initial offset  $\Delta_{init}$  (here 2 mm) of the ballast surface below each sleeper. The resulting irregularity in longitudinal level induces a pitching motion of the vehicle at the transition and increased dynamic loading of the track. In addition, the change of track form at the transition leads to a gradient in track stiffness at rail level. This leads to a further contribution to the transient excitation of the vehicle–track system and the differential settlement evolving in the ballasted track section.

The calculated time history of the vertical wheel–rail contact force is shown in Fig. 3 (top). Contributions to the dynamic load due to the stiffness gradient and the track irregularity at the transition zone can be observed. The sleeper–ballast contact forces along the ballasted track have also been calculated, see Fig. 3 (bottom). The sleeper–ballast contact force for sleepers close to the transition is higher than at sleepers farther away from the transition and exceeds the assumed threshold value. In this example, an initial threshold value of 62 kN has been assumed.

The calculated rail displacement (longitudinal level) after 50 MGT, when only accounting for the gravity load is presented in Fig. 4 (left). The influence of axle load on the magnitude of the uniform settlement ahead of the transition and the track irregularity at the transition is observed. As expected, when the sleeper–ballast contact force exceeds the initial threshold value, the dynamic loading will lead to differential settlement, and consequently to an irregularity in longitudinal level along the transition. Further, the vertical acceleration of sleepers along the transition have been computed, see Fig 4 (right). Here, it can be seen that sleeper acceleration near the transition is higher than elsewhere. In addition, it can be seen that the maximum vertical accelerations are obtained at similar locations as to where the maximum sleeper–ballast forces are computed.

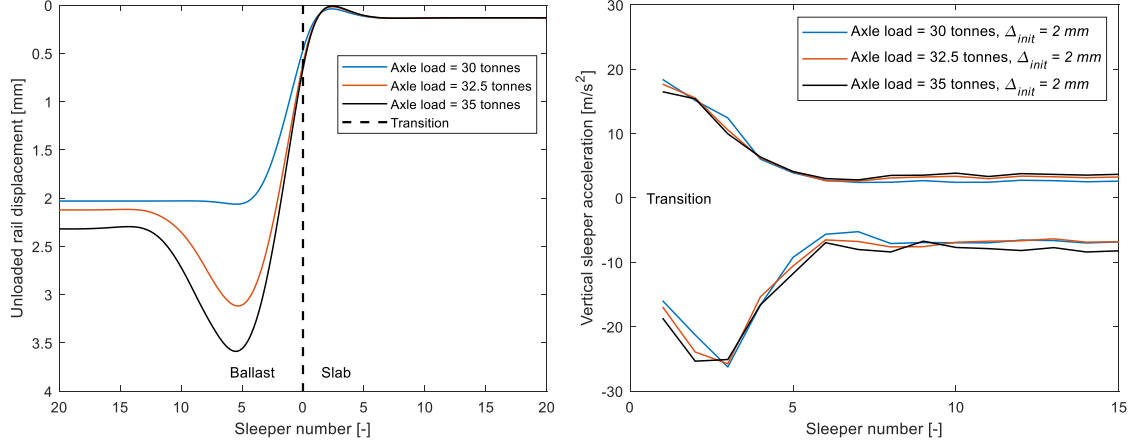


**Figure 4:** (left) Rail displacement due to gravity load after an accumulated traffic load of 50 MGT. Train speed 60 km/h and axle load 30, 32.5, or 35 tonnes. Results for  $\Delta_{init} = 2$  mm. (right) Maximum and minimum vertical sleeper acceleration along the transition zone. From (Nasrollahi et al., 2021).

#### 4. Instrumentation

To gather more insight into the performance of the transition zone, a monitoring programme has been designed that comprises both short-term and long-term measurements. The long-term measurements focus on capturing the track alignment (settlements), while the short-term measurements will be used to investigate the dynamic response, such as wheel–rail contact forces, sleeper–ballast forces, and sleeper displacements and accelerations.

To determine the vertical wheel–rail contact force between the two sleepers in a sleeper bay and the rail seat load on one sleeper, longitudinal strains at a given perpendicular distance ( $y$  in Fig. 5) from the neutral axis (N.A.) of the rail at four sections in one sleeper bay will be measured using an FBG strain array comprising four gauges. The strain range is  $\pm 1500 \mu\epsilon$ , while the operating temperature range is  $-20^\circ\text{C}$  to  $+60^\circ\text{C}$ . Based on Euler-Bernoulli beam theory, the relation between the strain  $\epsilon$  and the curvature of the rail is obtained (Eq. 1). Further, for a rail section with known bending stiffness (here  $EI = 6.4 \text{ MNm}^2$ ), the bending moment ( $M$ ) can be determined (Eq. 2). Next, by integrating the distributed force supporting the rail (Eq. 3) over the sleeper width  $s$  provides an estimate of the rail seat load (Eq. 4). Further, by substituting  $x = v \cdot t$  ( $v$  is vehicle speed) into (Eq. 1), it can be shown that the vertical acceleration  $a$  of the rail is determined by the curvature times the square of the speed (Eq. 5). The acceleration inferred from the strain can then be integrated twice with respect to time to obtain the deflection  $w(x)$  of the rail (Eq. 6) (Milosevic et al., 2021).

$$\kappa = \epsilon \cdot y = \frac{d^2 w(x)}{dx^2} \quad (1) \quad M(x) = EI \cdot \kappa \quad (2)$$

$$q(x) = \frac{d}{dx} Q(x) = \frac{d^2}{dx^2} (M(x)) \quad (3) \quad Q_s = \int_{-s/2}^{s/2} q(x) dx \quad (4)$$

$$\kappa = \epsilon \cdot y = \frac{d^2 w(x)}{d(vt)^2} \equiv \frac{a}{v^2} \quad (5) \quad w(t) = \iint_{t_1}^{t_2} a(t) dt \quad (6)$$

The instrumentation layout, based on FBG sensors, is presented in Fig. 5. FBG offers high sampling frequencies, a wide range of robust sensing options and immunity against electromagnetic interference (EMI). The optical fibre array is fixed to the bottom part of the rail web and can be interrogated using a single analyser. Each sensor

cluster consists of an array with four strain gauges with temperature compensation, one displacement transducer, and one accelerometer (two accelerometers at clusters one and four). Each sensor cluster is connected to one channel of the interrogator. Further, to measure the rail seat load and sleeper displacement at four positions along the transition zone, four individual fibre arrays (cluster) at four sleeper bays (sleeper bays number 2, 5, 8, and 11 from the transition) will be deployed.

The vertical sleeper displacement is assessed by using an optical displacement transducer that is placed on the sleeper end. The displacement range is  $\pm 50$  mm with a resolution of  $30 \mu\text{m}$ , and the operating temperature range is  $-20^\circ\text{C}$  to  $+60^\circ\text{C}$ . Sleeper displacement is measured relative to a fixed reference anchor in the ground at four positions along the transition zone: 1.2 m, 3.0 m, 4.8 m, and 6.0 m from the 3MB slab. Further, absolute sleeper vertical acceleration will be measured using an optical accelerometer to assess track deflection at the same four sleepers and at two reference points. One of the reference accelerometers is placed on top of the 3MB slab, while the other is placed far away from the transition zone (sleeper number 30 from the transition).

To develop a high precision and high-speed FBG-based optical sensing system, each sensor needs to be designed to have a high bandwidth response as part of the bandwidth budget available (which depends on the expected strain levels in each grating) and must be interrogated with high precision and with sufficiently high sampling frequency (obeying Nyquist frequency theory). At the same time, the interrogator should be able to interrogate multiple FBGs connected in series and multiplexed in the wavelength domain. This can be achieved by using a high-speed tuneable laser-based read-out system (Optics11 I4), referred to as the FAZT system. The FAZT optical interrogator is based on a semiconductor tuneable laser diode that has no moving parts, delivering a high level of reliability and accuracy in addition to a power and wavelength reference section that includes several fine and coarse periodic wavelength references (Karabacak et al., 2016).

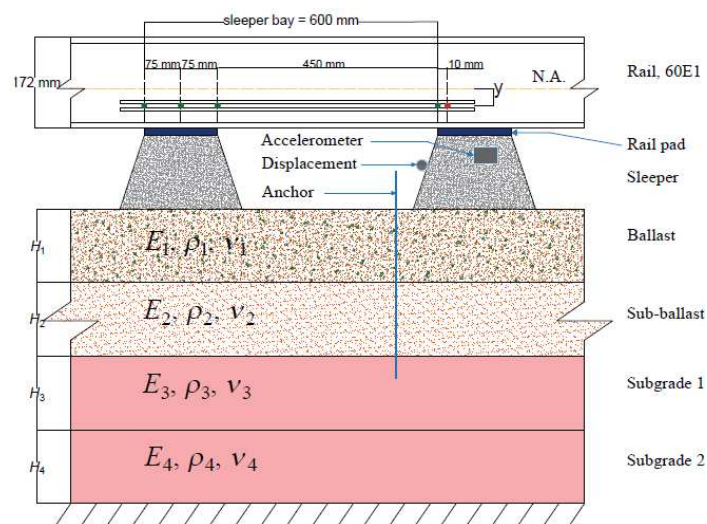


**Figure 5:** One cluster of sensors used for measurement of rail seat load, sleeper displacement and sleeper acceleration in one sleeper bay of the transition zone. It includes a FBG strain array on the rail web, one accelerometer on one sleeper, and one displacement transducer with an anchor used as reference.

Multiple levels of integrated wavelength referencing coupled with low-noise high-speed electronics allow for spectral feature tracking at a resolution of  $<20$  fm at kHz-frequencies. The unusually high sample frequency of  $f_s = 2$  kHz enables the current combination of (slowly evolving) static and dynamic measurements. The interrogator used has no moving parts resulting in high reliability over a broad temperature range and forms an integral part of a rugged and reliable sensing system. Using optical sensing gives the possibility to have kilometres of fibre between the readout and sensors, adding sensors without compromising measuring speed and resistance to EMI. The acquisition system comprises a computer, an I4 interrogator, a heated enclosure (to keep the logger within operational temperatures), a junction box, and 120 m optical fibres to transfer data from the sensors to the interrogator. The interrogator, which is connected to the rugged field computer in the heated enclosure, is continuously measuring all sensors at the pre-set fixed sampling frequency of 2 kHz and distributing those on a network socket. Subsequently, a custom script running on the field computer acquires the data from the interrogator, and formats and stores the data locally. The measurement script will be developed so that 'dynamic' snapshots, triggered by the far field accelerometer, are taken for each passing train and after post-processing (filtering, identification of the signal of interest) temporarily stored on the disk. Subsequently, these

data is synchronised with a server at Chalmers University of Technology. The expectation is that, given the amount of data obtained, size of the local storage on the field computer, quality of the telecommunication link (4g mobile data network), logarithmic nature of the degradation process, and total duration of the monitoring campaign, a trade off will be made on the measurement interval. That is, the number of dynamic snapshots at the start and near the end of the monitoring period will vary. Here, the ability for remote configuration of the system will help adapt to the needs of the project. Furthermore, data reduction techniques that only keep track of certain evolving (static and dynamic) metrics (peak force, displacement amplitudes, key frequencies, permanent displacement) rather than storing the complete signal for each train passage will be investigated after some data becomes available.

#### 4. Conclusions

This study has described the feasibility of FBG application for the SHM of a transition zone between two railway track forms in the north of Sweden. The FBG-based long-term monitoring arrangement, with a high temporal resolution, has been prepared to verify and calibrate a model for the prediction of settlement in a transition zone on the heavy haul line Malmbanan. Both long-term and short-term monitoring have been considered. The measurements will commence in September 2022.

#### Acknowledgements

The current study is part of the ongoing activities in CHARMEC–Chalmers Railway Mechanics ([www.chalmers.se/charmec](http://www.chalmers.se/charmec)). Parts of the study have been funded from the European Union's Horizon 2020 research and innovation programme in the projects In2Track2 and In2Track3 under grant agreement nos 826255 and 101012456. Discussions with Mr. Anders Karlsson and the Optics11 team are acknowledged.

#### References

- Du, C., Dutta, S., Kurup, P., Yu, T., and Wang, X. (2020). A review of railway infrastructure monitoring using fiber optic sensors. *Sensors and Actuators, A: Physical*, 303, 111728. <https://doi.org/10.1016/j.sna.2019.111728>
- Karabacak, D. M., Ibrahim, S. K., Koumans, Y., Meulblok, B., and Knoppers, R. (2016). High-speed system for FBG-based measurements of vibration and sound. *Fiber Optic Sensors and Applications XIII*, 9852, 98520I. <https://doi.org/10.1117/12.2223005>.
- Milosevic, M. D. G., Pålsson B. A., Nissen, A., Nielsen J. C. O., and Johansson, H. (2021). Reconstruction of sleeper displacements from measured accelerations for model-based condition monitoring of railway crossing panels, *submitted for international publication*, 26 pp.
- Morales-Gamiz, F. J. (2017). Design requirements, concepts and prototype test results for new system of ballast less system (3MB slab track), *Collaborative project SCP3-GA-2013-60560 Capacity4Rail (C4R), Increased Capacity 4 Rail (C4R) networks through enhanced infrastructure and optimised operations*, FP7-SST-2013-RTD-1.
- Nasrollahi, K., Nielsen, J. C. O., Aggestam, E., Dijkstra, J., and Ekh, M. (2021). Prediction of differential track settlement in transition zones using a non-linear track model. *Proceedings of the 27th IAVSD Symposium on Dynamics of Vehicles on Roads and Tracks*, St Petersburg (Russia) August 2021 (online conference).
- Nielsen, J. C. O. (2017). Track geometry degradation and track stiffness on Swedish railway lines, *Research report (2017:02)*, Department of Mechanics and Maritime Sciences, Chalmers University of Technology, Gothenburg, Sweden.
- Nielsen, J. C. O., Berggren, E. G., Hammar, A., Jansson, F., and Bolmsvik, R. (2020). Degradation of railway track geometry – Correlation between track stiffness gradient and differential settlement. *Proceedings of the Institution of Mechanical Engineers, Part F: Journal of Rail and Rapid Transit*, 234(1), 108–119. <https://doi.org/10.1177/0954409718819581>.
- Paixão, A. (2014). Transition zones in railway tracks: An experimental and numerical study on the structural behaviour, *PhD thesis*, Faculty of Engineering of University of Porto, Porto, Portugal.
- Trafikverket, (2020). Ytvågsseismik (MASW) Gransjö, Boden. Project number, 100322.
- Wang, P. (2015). Longitudinal force measurement in continuous welded rail with bi-directional FBG strain sensors. *Smart Materials and Structures*, 25(1). <https://doi.org/10.1088/0964-1726/25/1/015019>.
- Wang, H. (2019). Open aircraft performance modelling based on an analysis of aircraft surveillance data, PhD thesis, TU Delft University, Delft, Netherlands.
- Wheeler, L. N., Take, W. A., Hoult, N. A., and Le, H. (2019). Use of fiber optic sensing to measure distributed rail strains and determine rail seat forces under a moving train. *Canadian Geotechnical Journal*, 56(1), 1–13. <https://doi.org/10.1139/cgj-2017-0163>.

